Title	Optical second harmonic generation from Pt nanowires with boomerang-like cross-sectional shapes
Author(s)	Ogata, Yoichi; Nguyen, Anh Tuan; Miyauchi, Yoshihiro; Mizutani, Goro
Citation	Journal of Applied Physics, 110(4): 044301-1-044301-6
Issue Date	2011-08-16
Type	Journal Article
Text version	publisher
URL	http://hdl.handle.net/10119/10279
Rights	Copyright 2011 American Institute of Physics. This article may be downloaded for personal use only. Any other use requires prior permission of the author and the American Institute of Physics. The following article appeared in Yoichi Ogata, Nguyen Anh Tuan, Yoshihiro Miyauchi, and Goro Mizutani, Journal of Applied Physics, 110(4), 044301 (2011) and may be found at http://link.aip.org/link/doi/10.1063/1.3624593
Description	

Optical second harmonic generation from Pt nanowires with boomerang-like cross-sectional shapes

Yoichi Ogata, Nguyen Anh Tuan, Yoshihiro Miyauchi, and Goro Mizutani[a)]
School of Materials Science, Japan Advanced Institute of Science and Technology, 1-1 Asahidai, Nomi, Ishikawa 923-1292, Japan

We have fabricated Pt nanowires with boomerang-like cross-sectional shapes on the MgO(110) faceted template and observed their optical second-harmonic generation (SHG) response. In the TEM images the Pt nanowires on the MgO substrate had macroscopic C_{2v} symmetry, however, their structure had microscopic imperfections. In the SHG response, as a function of the sample rotation angle around the substrate normal, we found contributions from the nonlinear susceptibility elements χ_{113}, χ_{223}, χ_{311}, χ_{322}, and χ_{333} originating from the broken symmetry in the 3; [110] direction of the MgO substrate. The indices 1 and 2 denote the [001] and $[1\bar{1}0]$ directions, respectively. Under C_{2v} symmetry no SHG is expected in the *s*-in/*s*-out polarization configuration, however, a finite SHG was observed in this polarization configuration. We suggest that the SHG in the forbidden configuration might originate from the imperfections in the nanowire structure. © 2011 American Institute of Physics. [doi:10.1063/1.3624593]

I. INTRODUCTION

Recently, nanofabrication techniques have developed very rapidly. Optical second harmonic generation (SHG) spectroscopy is one of the tools used to characterize the fabricated nanostructures and has been used by researchers.[1,2] SHG is a coherent nonlinear optical process and its efficiency depends upon the symmetry of the geometrical structure of the medium. Metallic nanowires have interesting optical properties due to the strong anisotropy of their structures and the possible electronic confinement effect. Interesting applications to optical devices such as frequency converters are expected, using their nonlinear optical properties.[3]

The linear optical properties of several noble metal nanowires prepared by electron beam lithography were systematically investigated by Schider *et al*.[4] They found that the optical response of the noble metal nanowires was strongly dependent on the polarization of the light field. The polarization dependent plasmon excitation was judged to induce the enhancement of the local electric field intensity. On the contrary, the SHG properties of Au, Cu, and Pt nanowires with several nanometer widths prepared by shadow deposition method have been reported.[5–7] The SHG from Cu/Pt bimetallic nanowires have also been studied.[8] By using electromagnetic numerical simulation, SHG from metal nanocylinders was investigated in detail.[9] However, no attention has been paid to the correlation between the cross-sectional shapes of the nanowires and their SHG response as far as we know, except for the work we mention next.

Recently, Ogata *et al*. reported the relation between the cross-sectional TEM image of Pt nanowires prepared by shadow deposition from one grazing incident angle and their SHG response.[10] They reported that the cross-sectional shapes of the nanowires were considerably asymmetric. The template

MgO facets had cross-sections of saw-tooth shapes such as those in Fig. 1. The Pt nanowires were found to be formed on one side face of the facets. The cross-sectional shapes of the nanowires were similar to tilted ellipsoids, but parts of the Pt were seen to extend beyond the tops of the facets, as schematically shown by an arrow in Fig. 1. It was suggested that the platinum of these asymmetric parts might dominate the origin of the observed SHG. In order to gain further information about the origin of the SHG, it will be important to investigate nanowires with other cross-sectional shapes.

In this work, we attempted to control the cross-sectional shapes of the platinum near the tops of the facets of the MgO templates. Platinum was evaporated from two directions onto the faceted template, as shown in Fig. 2(a). In this way, the Pt nanowires on the two faces of the facets are connected at the tops of the faceted template and their cross-sections become symmetric with respect to the substrate normal, resembling 'boomerangs.' It is noted that the cross-sectional shapes still have asymmetry in the direction normal to the MgO substrate. We then compare the SHG efficiency of these nanowires with those of our previous work.[10] The effect of the difference of the cross section on the SHG response is discussed. By understanding the relation between geometrical
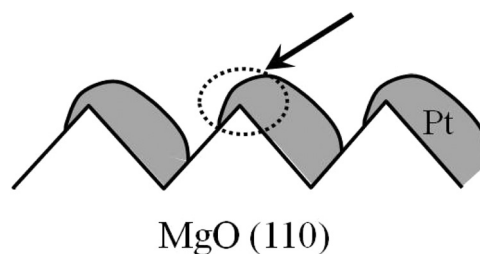

FIG. 1. The schematic cross-section of the nanowires deposited from one direction fabricated in our previous work (see Ref. 10). As indicated by an arrow, a part of the platinum is deposited on the top of the facets. Reprinted with permission from Y. Ogata *et al*., Surf. Interface. Anal. **42**, 1663 (2010).

---

a)Author to whom correspondence should be addressed. Electronic mail: mizutani@jaist.ac.jp.
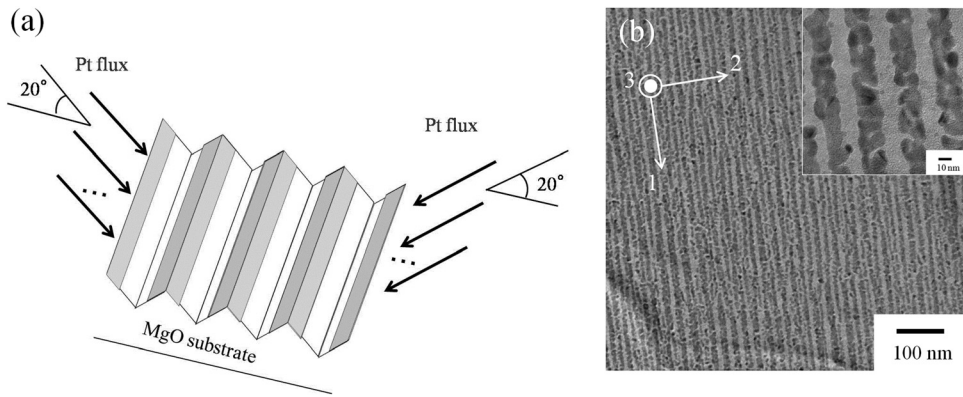
(a)

(b)

FIG. 2. (a) Schematic topography of faceted MgO (110) substrate with boomerang's cross-sectioned Pt nanowires fabricated by shadow deposition from two directions. (b) Pt nanowires observed by TEM and their expanded image (inset). Pt nanowires seen in the dark contrast run in direction 1; [001].

shapes of the cross sections and SHG response we expect we can control the SHG efficiency of the nanowires.

II. EXPERIMENTAL

Pt nanowires with the boomerang-like cross-sectional shapes on the faceted MgO(110) template were fabricated by the shadow deposition technique, as illustrated in Fig. 2(a), in a UHV chamber with a base pressure of 9.5×10^{-7} Pa.[10] The MgO substrate surface became faceted by self-organization with the periodicity depending on the homo-epitaxial growth. The facet formation of the surface was monitored by reflection high energy electron diffraction. The platinum was deposited at room temperature with a nominal thickness of 2 nm from two directions with an incident angle of 70° from the faceted MgO template normal, as shown in Fig. 2(a). According to the plan-view transmission electron microscope (TEM) images in Fig. 2(b), well-aligned Pt nanowires run along the [001] direction on the MgO(110) substrate. The minimum and maximum widths of the nanowires were 1.3 and 13.8 nm, respectively, and the average width was 7.1 nm. By depositing 5 nm thick SiO from the normal direction after the Pt deposition, the array of Pt nanowires on the template were protected.

In Fig. 2(b) we find many imperfections in the nanowires. If we increase the amount of Pt in order to remove these imperfections, it will then cause the nanowires touch their neighboring wires. Due to this trade-off, the nanowires in Fig. 2(b) are the best ones obtained for our present combination of the substrate and nanowire materials. Later in this paper these imperfections will be found to play an important role in the SHG response of the Pt nanowires.

The cross-sectional sample for the TEM observation was fabricated by an ion milling method. The Pt nanowires on the MgO(110) faceted template were first protected by epoxy resin. Subsequently, it was cut perpendicular to the wire axis by a dimple grinder. The (001) flake of MgO substrate was further ground by using an argon ion beam impinging normal to the flake face. The obtained thin MgO (001) flake with Pt nanowires was observed by TEM.

The measurement arrangement of the SHG has already been reported elsewhere.[10] To measure the SHG intensity from the Pt nanowire array, we used a frequency-doubled mode-locked Nd^{3+}: YAG laser at a photon energy of 2.33 eV with a pulse duration of 30 ps and a repetition rate of 10

Hz. The pulse energy was set at 120 μJ. The incident light was passed through a 2ω cut filter and a polarizer and the irradiated sample at an incidence angle of 45°. In order to measure the azimuthal angle dependence of the SHG intensity, the sample was mounted on a rotation stage. The reflected SHG light beam was passed through lenses, a polarizer, a ω cut filter, and a monochromator, and was detected by a photo-multiplier.

III. RESULTS AND DISCUSSION

Figure 3(a) shows a typical cross-sectional TEM image of the fabricated Pt nanowires on the MgO substrate. In Fig. 3(a), the platinum on the faceted MgO substrate resembles boomerangs. The Pt nanowires are seen to have a C_{2v} symmetry with a mirror plane in the 1-3 directions. Here, the numbers 1, 2, and 3 represent the [001], $[1\bar{1}0]$, and [110] directions on the MgO (110) template, respectively, as defined in Fig. 3(b).

In Figs. 4(a) to 4(d), we display the SHG intensity from the Pt nanowires such as those seen in Fig. 3(a), with empty circles as a function of the sample rotation angle, φ, around the substrate normal. The angle, φ, is defined as the angle between the incident plane and the [001] axis of the MgO(110) substrate, as illustrated in Fig. 3(b). The SHG intensity in Figs. 4(a) to 4(d) is strongly dependent upon the rotation angle, φ, for all polarization combinations. The pattern in the p-in/p-out polarization configuration in Fig. 4(a)
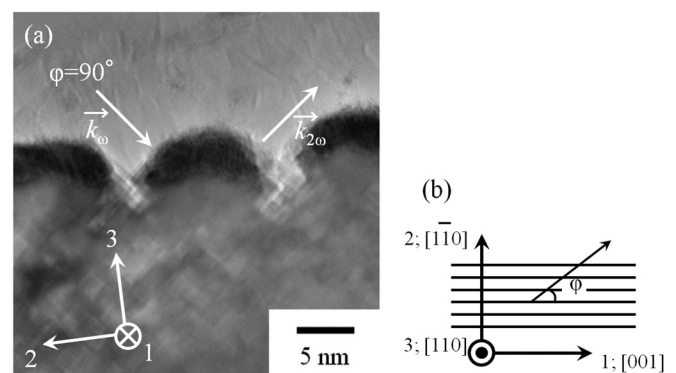

(a)

(b)

FIG. 3. (a) The cross-sectional shapes of the Pt nanowires on the MgO(110) faceted template observed by TEM. Two arrows show the wave vectors, $\vec{k}_{\omega}$ and $\vec{k}_{2\omega}$, of the fundamental and SHG light beams for $\varphi = 90°$, respectively. (b)The rotation angle, φ, defined as the angle between the plane of incidence and the direction 1; [001]; on the MgO (110) template.
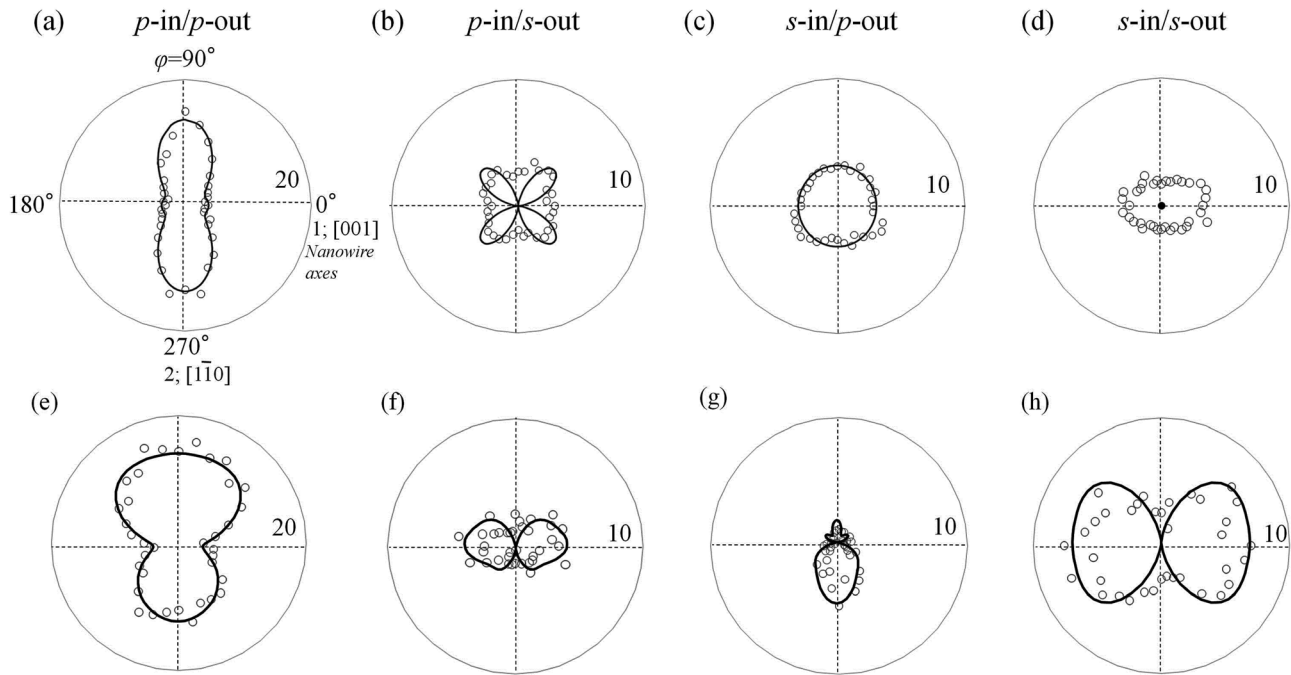
FIG. 4. Measured (empty circles) and calculated (solid line) SH intensity patterns for the (a)-(d) boomerang's, and (e)-(h) ellipsoid's cross-sectioned Pt nanowires/MgO (110) system in four different polarization configurations. The patterns (e)-(h) were reproduced from those published in Ref. 13. The relative SHG intensity is written in each chart. The four different polarization combinations are indicated at the top of each chart.

shows two-lobes at $\varphi = 90$ and $270°$. The one in the p-in/s-out polarization configuration in Fig. 4(b) shows a nearly isotropic response, but has four dim maxima at $\varphi = 45$, 135, 225, and $315°$. The one in the s-in/p-out polarization configuration in Fig. 4(c) is isotropic. The one in the s-in/s-out polarization configuration in Fig. 4(d) is elliptical with maxima at $\varphi = 0$ and $180°$. All of the patterns in Figs. 4(a) to 4(d) are symmetric with respect to the 0-180° axis line. Thus, the nanowires fabricated in this study have C_{2v} symmetry from a macroscopic point of view.

Previously, we obtained SHG patterns from the Pt nanowires with ellipsoidal cross–sections, as seen in Fig. 1.[13] We reproduce the SHG patterns in Figs. 4(e) to 4(h). In Fig. 1, a part of the Pt nanowires is seen to extend beyond the tops of the faceted MgO template. The edge of this extending part has local asymmetry and is C_s symmetric with a mirror plane in the 2-3 directions. Thus, the SHG patterns show two unequal lobes at $\varphi = 90$ and $270°$ for p-in/p-out (Fig. 4(e)), two small lobes at $\varphi = 0$ and $180°$ for p-in/s-out (Fig. 4(f)), one main lobe at $\varphi = 270°$ for s-in/p-out (Fig. 4(g)), and two lobes at $\varphi = 0$ and $180°$ for s-in/s-out (Fig. 4(h)). The SHG patterns in Figs. 4(a) to 4(d) are remarkably different from those in Figs. 4(e) to 4(h). This fact simply shows that the control of the cross-sections of the Pt nanowires has led to the change in the nonlinear optical properties of the nanowires.

The SHG intensity patterns in Fig. 4 have been analyzed phenomenologically following the analyses by previous authors.[6,11] We first calculated the SHG intensity patterns for each nonlinear optical susceptibility element by using Maxwell's equations. The nonlinear polarization, P_i^{NL}, induced in the nanowire array at the second-harmonic frequency can be written as

$$P_i^{NL} = \varepsilon_0 \sum_{j,k} \chi_{ijk}^{(2)} E_j^\omega E_k^\omega. \qquad (1)$$

Here, $\chi_{ijk}^{(2)}$ is a third-rank tensor of the second-order nonlinear susceptibility of the nanowire array. The electric field, E, in the nanowire array at the fundamental frequency on the right-hand side of Eq. (1) was calculated by Maxwell's equations, assuming the nanowire array as a flat thin dielectric slab. The output electric field at the second harmonic frequency was calculated by Maxwell's wave equations with Eq. (1) as the source term. Thus the total SHG intensity was a linear combination of these SHG intensity patterns with each term multiplied by the corresponding nonlinear susceptibility element. Finally, these total SHG intensity patterns were fitted to the experimental patterns in Fig. 4 by varying each nonlinear susceptibility element as fitting parameters.

We tried to fit the theoretical SHG intensity patterns to the experimental data in Figs. 4(a) to 4(d) by assuming C_{2v} symmetry for the Pt nanowires with boomerang shapes on the MgO(110) faceted face. Under C_{2v} symmetry, there are five nonzero nonlinear susceptibility elements: χ_{113}, χ_{223}, χ_{311}, χ_{322}, and χ_{333}. In Fig. 4 we show the best fit calculated patterns in solid curves. In Fig. 5 the total calculated SHG intensity is decomposed into the contributions of different nonlinear susceptibility elements.

Let us first look at the SHG pattern in the p-in/p-out polarization configuration in Fig. 4(a). In Fig. 4(a) the SHG intensity is high at $\varphi = 90$ and $270°$. In Fig. 5(a) the contribution of the nonlinear susceptibility elements have a relation as $|\chi_{223}| \gg |\chi_{113}|$, and χ_{223} dominates the SHG intensity pattern shape in the p-in/p-out polarization configuration. This relation is consistent with the fact that the nanowires have a boomerang's cross-section in the 2-3 plane. This

(a)

ijk	p-in/p-out	p-in/s-out	s-in/p-out	s-in/s-out
113	·	·		
223	(pattern)	(pattern)		
311	(pattern)			(pattern)
322	(pattern)		(pattern)	
333	·			

(b)

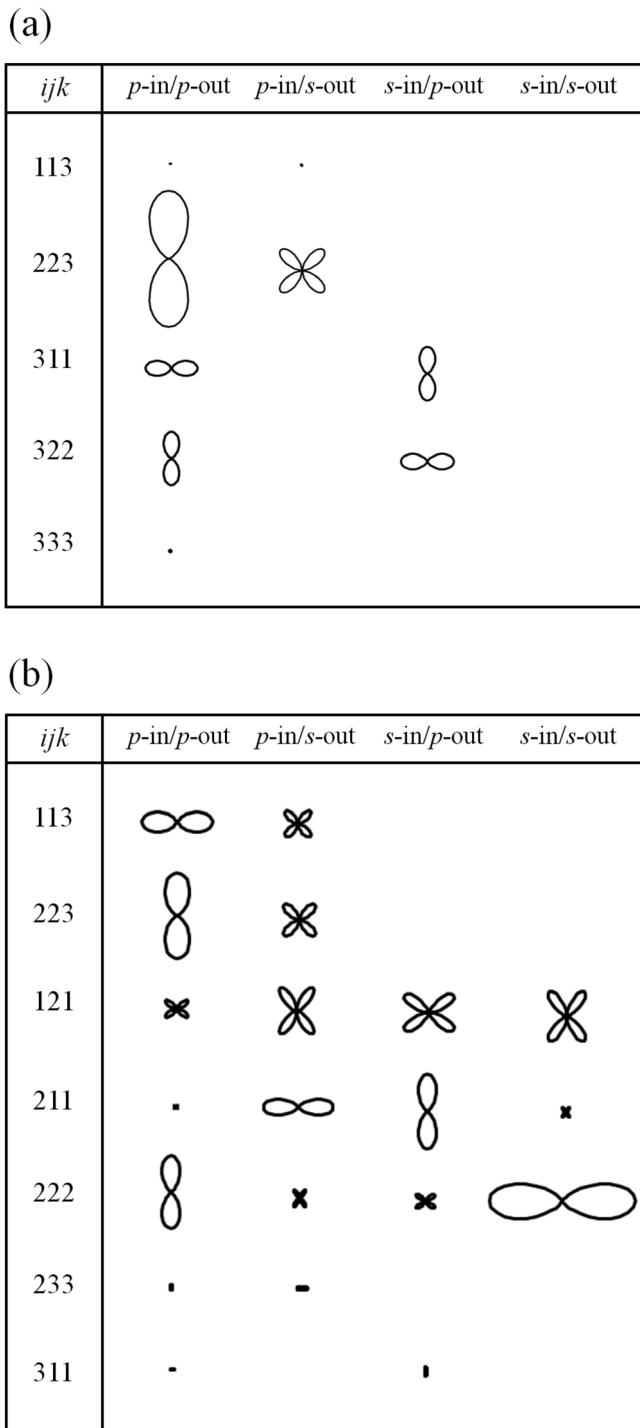| ijk	p-in/p-out	p-in/s-out	s-in/p-out	s-in/s-out
113	(pattern)	(pattern)		
223	(pattern)	(pattern)		
121	(pattern)	(pattern)	(pattern)	(pattern)
211	·	(pattern)	(pattern)	×
222	(pattern)	×	×	(pattern)
233	·	–		
311	–		(pattern)	

FIG. 5. The SHG intensity patterns from Pt nanowires decomposed into the contributions of the nonlinear susceptibility elements. The intensities in the polar directions are in arbitrary but common units. (a) Data in Figs. 4(a) to 4(d) decomposed under C_{2v} symmetry, and (b) those in Figs. 4(e) to 4(h) decomposed under C_s symmetry.

cross-sectional shape causes the motion of electrons in the 2 and 3 directions to mix with each other and produces the observed optical nonlinearity. On the contrary, the nanowire has a translational symmetry in the 1 direction and the optical nonlinearity, χ_{113}, is not large.

The nonlinear optical susceptibility element, χ_{223}, should also produce the four-fold symmetric SHG intensity pattern in the p-in/s-out polarization configuration, as seen in Fig. 5(a), although the calculation does not completely reproduce the experiment, as seen in Fig. 4(b). In Fig. 5(a) we find that the contribution of the nonlinear susceptibility of χ_{322} and χ_{311} are of the same magnitude. This makes the SHG intensity pattern isotropic in the s-in/p-out polarization configuration, as seen in Fig. 4(c). As a result, the contributions of the χ_{113}, χ_{223}, χ_{311}, and χ_{322} elements are proved to be dominant in p-in/p-out, p-in/s-out, and s-in/p-out polarization configurations. These nonlinear susceptibility elements occur due to the broken symmetry in direction 3.

Conversely, the theoretical SHG intensity pattern with C_{2v} symmetry did not reproduce the experimental data in the s-in/s-out polarization configuration. Namely, every allowed nonlinear optical susceptibility element under C_{2v} symmetry gives zero SHG intensity in the s-in/s-out polarization configuration, as seen in Fig. 5(a), although the experimental result in Fig. 4(d) shows nonzero SHG intensity. According to our previous report,[10] the nonlinear optical susceptibility element, χ_{222}, makes a SHG intensity pattern with two lobes at $\varphi = 0$ and 180° in the s-in/s-out polarization configuration as seen in Fig. 4(h). In Ref. 10, parts of the platinum extending beyond the tops of the facets, as seen in Fig. 1, were suggested to generate the optical nonlinearity in direction 2 and to make the element, χ_{222}, nonzero.

For the sample in the present study, we intended to remove this asymmetry of the platinum shape in direction 2 at the tops of the MgO facets by depositing the platinum from two directions. Thus, the nonlinear susceptibility element, χ_{222}, was expected to be zero. Contrary to this expectation, we see nonzero SHG intensity for the s-in/s-out combination with peaks at $\varphi = 0$ and 180°, as seen in Fig. 4(d). Even so, the SHG intensity ratio, I_{ss}/I_{pp}, for the boomerang nanowires was 0.48 times that of the nanowires of our previous paper.[13] This relatively small SHG intensity in the s-in/s-out polarization configuration is roughly consistent with the expectation.

As the candidate origin of the remaining SHG intensity in the s-in/s-out polarization configuration, the imperfections of the shapes of the nanowires is suggested. In order to clarify the validity of this candidate origin, we observed the TEM images again in more detail. Among the TEM images we found asymmetric boomerang-shaped platinum cross sections, as shown in Figs. 6(a) and 6(b). Approximately 30% of the examined nanowire cross sections had such
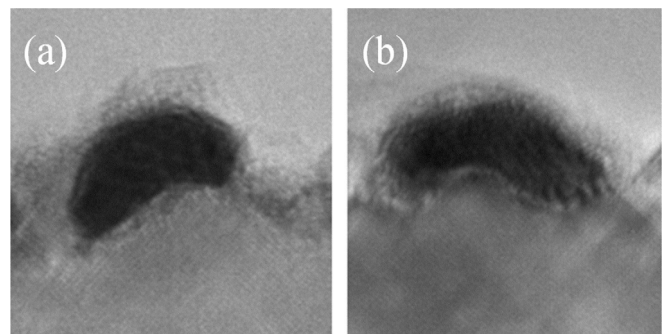

FIG. 6. Partial cross-sectional TEM images of Pt nanowires showing asymmetric boomerang shapes. These asymmetric boomerang shapes are seen at 30% of all nanowires.

asymmetric boomerang cross-sections. Nonlinear polarizations, P_2^{NL}, induced by the incident electric field in direction 2 at the cross-sections such as those in Figs. 6(a) and 6(b) should have opposite signs to each other. The spatial separation of the SHG from these two kinds of structures is not possible because the beam size of ∼1 mm used in the SHG experiment is much larger than the size of each structure. Statistically, the reflected SH light from these two kinds of structures should cancel each other if we assume a random distribution. However, the fact that SHG is observed in Fig. 4(d) indicates that the cancellation of the SHG from the two types of the asymmetric nanowires was incomplete.

We can consider the effect of platinum nanodots on the SHG intensity patterns. Kitahara *et al.* reported isotropic SHG in the *p*-in/*p*-out and *s*-in/*p*-out polarization configurations from Au nanodots on the NaCl(110) faceted templates.[5] Therefore, there can be a contribution of the Pt nanodots in the *p*-in/*p*-out and *s*-in/*p*-out polarization configurations in Fig. 4, but not in the *s*-in/*s*-out polarization configuration.

Next, we consider the polarization scrambling of the light field, induced by the roughness of the nanowire structures seen in Fig. 2(b). Mills *et al.* have discussed the general effect of the roughness of metal surfaces on the optical processes upon them.[12] Using their formalism, we consider the conversion of *s*-polarized light into *p*-polarized light due to the roughness of the nanowire structure used here.

We consider the conversion of the *s*-polarized incident field of frequency, ω, by the roughness, $\zeta(x,y)$, of the metal nanowire structure. Here, $\zeta(x,y)$ represents the deviation of the height of the metal surface of the nanowires from that of the ideal ones. We consider the case of $\varphi = 0°$ so that the wave vector component of the incident light parallel to the substrate is in direction 1. The electric field of the *s*-polarized incident light is in direction 2. The electric field, $\vec{E}_{NF}^{\omega}$, near the nanowire is generally expanded with respect to $\zeta(x,y)$ as,

$$\vec{E}_{NF}^{\omega} = E_2^{\omega}\vec{e}_2 + \varsigma(x,y)(c_{21}^{(1)}\vec{e}_1 + c_{23}^{(1)}\vec{e}_3)E_2^{\omega} + \varsigma(x,y)^2(c_{21}^{(2)}\vec{e}_1 + c_{23}^{(2)}\vec{e}_3)E_2^{\omega}. \quad (2)$$

Here, $C_{jk}^{(i)}$ is a coefficient describing the rate of the conversion of the *j*-polarized electric field into the *k*-polarized one, and $\vec{e}_1$ and $\vec{e}_2$ are unit vectors in the 1 and 2 directions, respectively. Averaging Eq. (2) over the area on the substrate of a wavelength size, the second term vanishes and Eq. (2) becomes

$$\langle \vec{E}_{NF}^{\omega} \rangle = E_2^{\omega}\vec{e}_2 + \langle \varsigma(x,y)^2 \rangle(c_{21}^{(2)}\vec{e}_1 + c_{23}^{(2)}\vec{e}_3)E_2^{\omega}. \quad (3)$$

On the contrary, the contribution of the nonlinear optical susceptibility element, $\chi_{223}^{(2)}$, was dominantly responsible for the enhancement of the SH intensity at $\varphi = 90$ and $270°$ in the *p*-in/*p*-out polarization configuration as seen in Fig. 5(a). This nonlinear susceptibility element yields a nonlinear polarization,

$$P_2^{NL} = \varepsilon_0\chi_{223}^{(2)}E_2^{\omega}E_3^{\omega}. \quad (4)$$

Substituting the 3-component of Eq. (3) for E_3^{ω} in Eq. (4), we obtain,

$$P_2^{NL} = \varepsilon_0\chi_{223}^{(2)}E_2^{\omega}\langle E_{NF3}^{\omega}\rangle,$$
$$= \varepsilon_0\chi_{223}^{(2)}E_2^{\omega}\langle \varsigma(x,y)^2 \rangle c_{23}^{(2)}E_2^{\omega}. \quad (5)$$

Equation (5) indicates that the roughness on the nanowires generates the SHG in the *s*-in/*s*-out polarization configuration. If $C_{23}^{(2)}$ is weakly dependent upon the direction of the electric field, the SHG intensity in *s*-in/*s*-out is high when the incident electric field is in direction 2. In this configuration, φ is 0 or 180°. This is consistent with the pattern observed in Fig. 4(d).

The discrepancy between the experimental SHG data and theoretical pattern seen in Fig. 4(b) may also be ascribed to the imperfection of the nanowire structures. Namely, in the inset of Fig. 2(b), we see slight local undulation of the Pt nanowires in the several nanometer scale. This undulation of the nanowires should add an isotropic SHG component to the pattern. Namely, the undulation compromises the directionality of the nanowire axes and disturbs the SHG intensity pattern in Fig. 4(b). However, a quantitative analysis of this pattern change will require more detailed models.

IV. CONCLUSION

We have evaporated platinum from two directions onto faceted MgO(110) templates. According to the TEM observation, the cross-sections of the platinum nanowires resembled boomerangs. From their SHG intensity patterns, the nonlinear susceptibility elements corresponding to the C_{2v} symmetry of the nanowire structure were identified. We have concluded the fact that the control of the nanowires' cross-sections has led to the change in their nonlinear optical property. For the nanowires with C_{2v} symmetry and the boomerang's cross-sections, the nonlinear susceptibility elements χ_{113}, χ_{223}, χ_{311}, and χ_{322}, due to the broken symmetry in direction 3, dominate the SHG signal in the *p*-in/*p*-out, *p*-in/*s*-out, and *s*-in/*p*-out polarization configurations. The SHG signals observed in the *s*-in/*s*-out polarization configuration are suggested to originate from the imperfection of the nanowire structure.

[1]S. W. Liu, H. J. Zhou, A. Ricca, R. Tian, and M. Xiao, Phys. Rev. B **77**, 113311 (2008).
[2]H. M. Su, J. T. Ye, Z. K. Tang, and K. S. Wong, Phys. Rev. B **77**, 125428 (2008).
[3]J. C. Johnson, H. Yan, R. D. Schaller, P. B. Petersen, P. Yang, and R. J. Saykally, Nano Lett. **2**, 279 (2002).
[4]G. Schider, J. R. Krenn, W. Gotschy, B. Lamprecht, H. Ditlbacher, A. Leitner, and F. R. Aussenegg, J. Appl. Phys. **90**, 3825 (2001).

[5]T. Kitahara, A. Sugawara, H. Sano, and G. Mizutani, Appl. Surf. Sci. **219**, 271 (2003).

[6]K. Locharoenrat, H. Sano, and G. Mizutani, J. Lumin. **128**, 824 (2008).

[7]N. Hayashi, K. Aratake, R. Okushio, T. Iwai, H. Sano, A. Sugawara, and G. Mizutani, Appl. Surf. Sci. **253**, 8933 (2007).

[8]N. A. Tuan and G. Mizutani, e-J. Surf. Sci. Nanotechnol. **7**, 831 (2009).

[9]C. G. Biris and N. C. Panoiu, Phys. Rev. B **81**, 195102 (2010).

[10]Y. Ogata, N. A. Tuan, S. Takase, and G. Mizutani, Surf. Interface. Anal. **42**, 1663 (2010).

[11]E. Kobayashi, G. Mizutani, and S. Ushioda, Jpn. J. Appl. Phys. **36**, 7250 (1997).

[12]A. A. Maradudin and D. L. Mills, Phys. Rev. B **11**, 1392 (1975).

[13]Y. Ogata, N. A. Tuan, S. Takase, and G. Mizutani, J. Surf. Anal. **17**, 252 (2011).